Thin Solid Films 519 (2011) 5353–5357

Contents lists available at ScienceDirect

Thin Solid Films

journal homepage: www.elsevier.com/locate/tsf

AlTiN layer effect on mechanical properties of Ti-doped diamond-like carbon composite coatings

Xiaolu Pang [a], Huisheng Yang [a,*], Kewei Gao [a], Yanbin Wang [a], Alex A. Volinsky [b]

[a] Department of Materials Physics and Chemistry, University of Science and Technology Beijing, Beijing 100083, China
[b] Department of Mechanical Engineering, University of South Florida, Tampa FL 33620, USA

ARTICLE INFO

Article history:
Received 28 December 2009
Received in revised form 9 February 2011
Accepted 11 February 2011
Available online 24 February 2011

Keywords:
Interlayer
DLC
AlTiN
Tribology
Adhesion

ABSTRACT

Ti/Ti-doped diamond-like carbon (DLC) and Ti/AlTiN/Ti-DLC composite coatings were deposited by magnetron sputtering on W18Cr4V high speed steel substrates. The effect of the AlTiN support layer on the properties of these composite coatings was investigated through microstructure and mechanical properties characterization, including hardness, elastic modulus, coefficient of friction and wear properties measured by scanning electron microscopy, Raman spectroscopy, scratch and ball-on-disk friction tests. Ti and AlTiN interlayers have a columnar structure with 50–80 nm grains. The hardness and elastic modulus of Ti/Ti-DLC and Ti/AlTiN/Ti-DLC coatings is 25.9 ± 0.4, 222.2 ± 6.3 GPa and 19.3 ± 1, 205.6 ± 6.7 GPa, respectively. Adhesion of Ti-DLC, Ti/AlTiN/Ti-DLC and AlTiN/Ti-DLC coatings expressed as the critical lateral force is 26.5 N, 38.2 N, and 47.8 N, respectively. Substrate coefficient of friction without coatings is 0.44, and it is 0.1 for Ti/Ti-DLC and Ti/AlTiN/Ti-DLC coatings. Wear resistance of Ti/AlTiN/Ti-DLC composite coatings is much higher than Ti/Ti-DLC coatings based on the wear track width of 169.8 and 73.2 μm, respectively, for the same experimental conditions.

1. Introduction

With the fast development of coating technology, single layer coatings no longer satisfy industrial requirements, thus double or combination coatings and multilayers have been developed as a new generation of protective coatings [1–3]. Diamond-like carbon (DLC) is one of the best coatings with high hardness, optical transparency in the visible and infrared regions, high electrical and thermal conductivities, high wear resistance and excellent biocompatibility [3–5]. All of these properties allow for important applications and encourage research works to develop techniques and methods to deposit this kind of films. DLC coatings usually consist of amorphous material with a combination of graphite-like sp^2 and diamond-like sp^3 bonds. However, the problem of low adhesion resulting from a high level of internal stress in DLC films and thermal expansion mismatch when grown on substrates such as high speed and stainless steels, has restricted their use. Adhesion improvement routes have been studied along with the problem of coating thermal stability. Adding a metal interlayer between DLC coating and the substrate, and doping DLC with metal have been utilized to solve this problem [6–8]. Metal-containing diamond-like carbon (Me-DLC) is a DLC film in which nano-scale metal clusters are dispersed homogeneously helping to solve adhesion problems. Metal clusters are remarkably effective for decreasing the stress in DLC films. Tribological properties of Me-DLC films in dry sliding wear using a ball-on-disk tribometer have been reported [9,10]. The average friction coefficient strongly depends on the test duration [11–13]. The wear rate correlates with both hardness and with the intrinsic nanometer-scale roughness of Me-DLC [11]. Friction and sliding characteristics of Me-DLC have been studied [14–16], with a possibility of non-lubricated sliding. However, DLC thin film hardness generally drops with an increased amount of metal inclusions, and film damage occurs rather than delamination.

Another way to solve adhesion problems is to add an interlayer between the substrate and the Me-DLC coating. AlTiN coating has been proven to increase the cutting performance in heavy duty machining of hardened or austenitic stainless steels. These advantages are observed in different cutting operations like milling, turning, or drilling. Strong improvements of operational properties are directly connected with smooth surface, high hardness, and very good adhesion. For applications where low friction is favorable, AlTiN can be combined with a Ti–C:H top layer [17].

In this work we studied and compared properties of Ti-DLC and Ti/AlTiN/Ti-DLC coatings deposited on the high speed steel substrates (HSS). Using specific analytical methods, microstructure and mechanical properties, including hardness, elastic modulus, and coefficient of friction, and wear properties were investigated by scanning electron microscopy, Raman spectroscopy, and scratch and ball-on-disk friction tests.

2. Experimental details

Ti/AlTiN/Ti-DLC and Ti/Ti-DLC composite coatings were deposited by magnetron sputtering (Ti/AlTiN) and plasma-enhanced chemical

* Corresponding author. Tel.: +86 10 82376048; fax: +86 10 62334909.
E-mail address: pangxl@mater.ustb.edu.cn (H. Yang).

0040-6090/$ – see front matter
doi:10.1016/j.tsf.2011.02.040

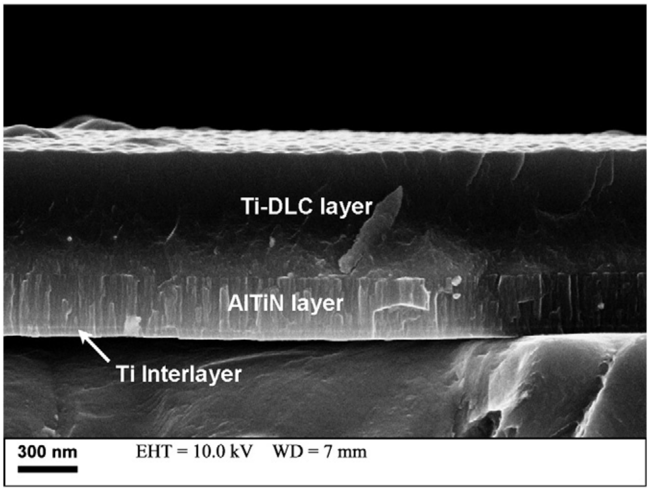

Fig. 1. Cross-section SEM micrograph of Ti/AlTiN/Ti-DLC composite coatings.

vapor deposition (Ti-DLC) on the high speed steel W18Cr4V, which is widely used in die and cutting tools (C: 0.7–0.8%, W: 17.8–19%, Cr: 3.8–4.4%, V: 1.0–1.4%, Si: ≤0.4%, Mn: ≤0.4%, Mo:≤0.3%). Ti and metallic compound targets (Al/Ti at.% ratio = 33:67) with a purity of 99.9% were used. One of the two sources was used to deposit the Ti interlayer between the substrate and the main layer to improve adhesion. The second AlTi target was employed to deposit the AlTiN layers. An ion source was utilized to enhance ion intensity. The rotation speed of the substrate holder was 30 rpm. The target current was 1 A, the base pressure was 2×10^{-4} Pa, and the flow rate of Ar with 99.99% purity was 45 standard cubic centimeters per second (sccm), while the reactive gas was N_2 with 99.99% purity. After Ti/AlTiN deposition, C_2H_2 was introduced into the chamber for Ti-DLC deposition with a self bias of −400 V.

Prior to sputtering, substrates were cleaned in acetone and ethanol for 10 min, respectively, and subjected to 10 min in-situ Ar plasma cleaning at RF power of 100 W in order to remove any contaminants on the substrate surface and to activate the surface. Ti interlayer was deposited on the substrates for 5 min with a DC current of 1 A, and then N_2 gas was introduced into the sputtering chamber.

Microstructure of composite coatings was characterized by cross-section scanning electron microscopy (Zeiss Supra™ 55) with a 10.0 kV operating voltage and Raman spectroscopy (Jobin-Yvon HR-800). Hardness and Young's modulus of the coatings were characterized using Hysitron Triboindenter with a Berkovich diamond indenter tip. Hardness and modulus values presented are maximum average values from 9 indentations on each sample in the 70–80 nm depth range. Hardness values were obtained by analyzing the unloading portion of the load-displacement curves using the Oliver–Pharr method varying with indentation depth.

Adhesion and tribological properties of composite coatings were evaluated by means of scratch and ball-on-disk tests using a Micro-Tribometer model UMT-2 at room temperature in air, made by the Center for Tribology Inc. Normal load was continuously increased at a rate of 1 N/s, while the conical diamond tip (120° angle, 200 μm tip

Table 1
Ti-DLC layer elemental composition.

Element	Weight %	Weight % error	Atom %	Atom % error
C	81.91	±2.71	94.45	±3.12
Al	1.79	±0.18	0.92	±0.09
Ti	14.37	±0.55	4.15	±0.16
Fe	1.93	±0.31	0.48	±0.08
Total	100.00		100.00	

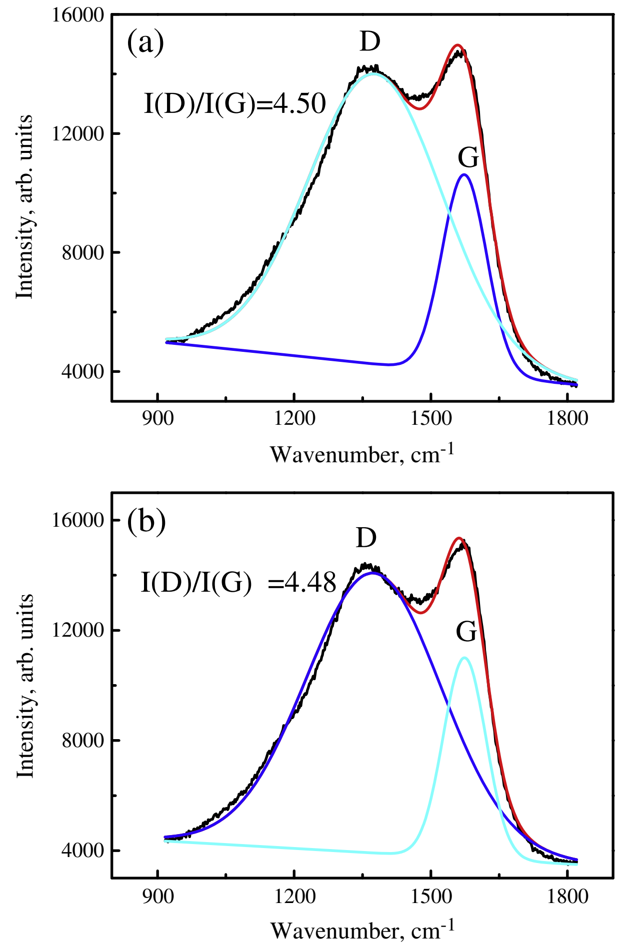

Fig. 2. Raman spectrum of the DLC layer of (a) Ti/Ti-DLC and (b) Ti/AlTiN/Ti-DLC coatings.

radius) was moving at a constant velocity of 0.05 mm/s for adhesion test. GCr15 steel ball with high carbon and chrome contents (C: 0.95–1.05%, Mn: 0.25–0.45%, Si: 0.15–0.35%, S: ≤0.025%, P: ≤0.025%, Cr: 1.40–1.65%, Mo: ≤0.10%, Ni: ≤0.30%, Cu: ≤0.25%, Ni + Cu: ≤0.50%) was used to characterize coating wear properties in air. A normal load of 10 N was applied to the coating surface for 1 h. The circular wear track developed on the coating had a radius of 6 mm, and the ball rotational speed was 600 rpm.

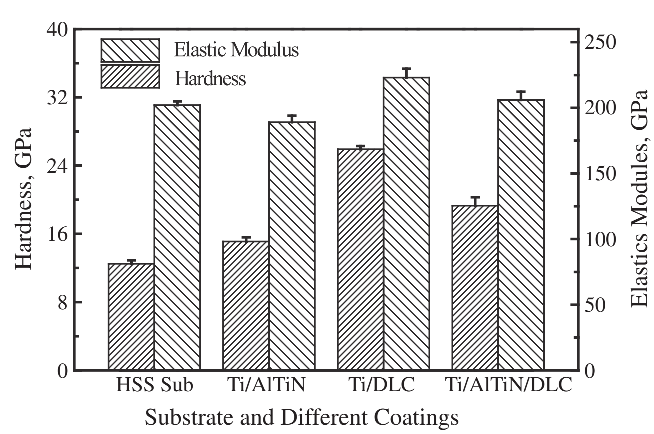

Fig. 3. Hardness and elastic modulus of the steel substrate, Ti/AlTiN, Ti/Ti-DLC and Ti/AlTiN/Ti-DLC coatings.

3. Results and discussion

Fig. 1 shows the scanning electron microscope (SEM) cross-section of the Ti/AlTiN/Ti-DLC composite coatings, including the interfaces. Coatings are quite dense with no pores or inclusions present. While stresses in each layer are independent, several studies show that a metal interlayer, 0.5–1.5 μm thick helps to accommodate coating residual stresses and allows for a thicker coating to be produced, with significant improvements in toughness, adhesion and impact resistance [18–20]. Fig. 1 also shows the microstructure of Ti interlayer and AlTiN layer with columnar 50–80 nm grains, and the thickness of Ti, AlTiN and DLC layers is about 70, 300, 800 nm, respectively. Interfaces between Ti/substrate and AlTiN/DLC layers are clearly identified in Fig. 1 with dense and very thin amorphous layer. Maximum deposition temperature of Ti/Ti-DLC and Ti/AlTiN/Ti-DLC coatings was about 60 °C and 72 °C, respectively. Table 1 shows the elemental analysis of Ti-DLC layer obtained from energy dispersive spectra. The amount of Ti in DLC layer is about 4.15 at.%.

Fig. 2 shows the typical deconvoluted Raman spectra fitted with Gaussians. Raman spectra have a relatively sharp peak at approximately 1578 cm^{-1} and a broadening peak at approximately 1380 cm^{-1}, commonly referred to as the G and D bands, which correspond to diamond sp^3 and graphite sp^2 bonds, respectively. The latter is wider and blunter than the former one because the film is hydrogenated and

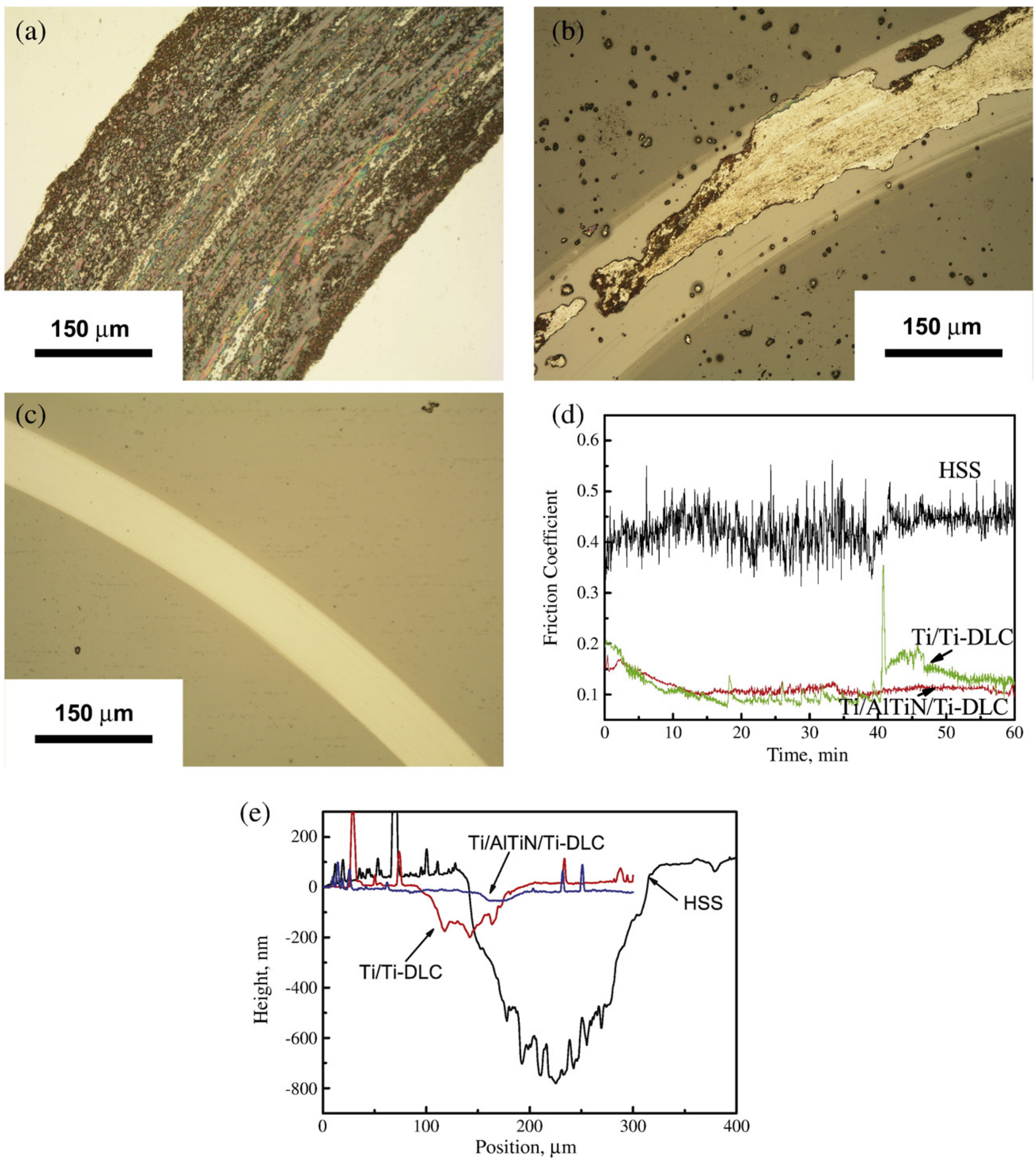

Fig. 4. Wear and friction tests of the substrate, Ti/Ti-DLC and Ti/AlTiN/Ti-DLC coatings. (a) The substrate; (b) Ti/Ti-DLC coatings; (c) Ti/AlTiN/Ti-DLC coatings; (d) Friction coefficient; (e) Profiles of wear scars.

the content of graphite is much higher. The shift of both G or D peaks and their intensity ratio change, I(D)/I(G), mean that the size of the crystal cluster changed. Generally, with the crystal cluster size decreasing, the peak shifts to a higher wave number. In this experiment, the value of the I(D)/I(G) ratio shows a slight decrease from Fig. 2(a) to Fig. 2(b), which can be qualitatively descriptive of more sp^3 bonds. Based on Eq. (1), the cluster size could be increasing as well. The peak width and intensity ratio both vary depending on the DLC film structure. Cluster size can be calculated using Landford's function [21]:

$$I(D)/I(G) = (-126 + 0.033\lambda)/L_a \quad (1)$$

where λ and L_a are the laser wavelength and cluster size, respectively. The value of I(D)/I(G) changes and coating microstructure also has a contribution to this change.

Fig. 3 shows the hardness and elastic modulus of high speed steel substrate, Ti/AlTiN, Ti/Ti-DLC, and Ti/AlTiN/Ti-DLC composite coatings, respectively. In composite coating system, hardness is influenced by both the film and the substrate. Buckle et al. proposed that the composite hardness H_c of a bilayer material could be expressed as [22,23]:

$$H_c = aH_f + bH_s \quad \text{with } a + b = 1. \quad (2)$$

where a varies from 1 to 0, when the hardness is not substrate-dependent and when the thickness of the coating is negligible compared with the indentation depth. Based on this formula, hardness of composite coating is in the range between the hardness of different layers. In our case, hardness of the top Ti-DLC layer is 25.9 GPa, and of the support AlTiN layer is 15.1 GPa, so the composite hardness is 19.3 GPa. X-ray reflectivity experiments were performed on DLC layers and show that the density of DLC films changes from 1.8 to 2.1 g/cm^3. The density and hardness of DLC films increase with sp^3 bond content in all kinds of amorphous carbon films, which was discussed by Ferrari and Robertson [24,25].

Fig. 4 shows the wear scars of the substrate and composite coatings after 1 hour wear test under the 10 N normal load. Fig. 4(a) shows that the surface of HSS substrate sustained serious damage with a 416.5 μm wide wear scar. Fig. 4(b) and (c) shows Ti/Ti-DLC and Ti/AlTiN/Ti-DLC coatings' surfaces after wear test. Fig. 4(b) shows that the Ti/Ti-DLC coatings partly delaminated from the substrate with a sharp decrease of the wear scar width to 169.8 μm. In Fig. 4(c) there is a wear scar of Ti/AlTiN/Ti-DLC coatings with a width of 73.2 μm and there is no coating delamination present in the wear scar. Compared with Fig. 4(b) and (c), the wear volume loss is higher for Ti/Ti-DLC coatings, signified by a deeper cross-sectional profile in Fig. 4(e). The width and depth of HSS substrate wear scar are much wider and deeper than the Ti/Ti-DLC coating wear scar, and the width and depth of Ti/Ti-DLC coatings are wider and deeper than the Ti/AlTiN/Ti-DLC coatings wear scar.

Ball-on-disk test was used to obtain the friction coefficient of substrate and coatings by measuring the lateral force during sliding contact. Fig. 4(d) shows the substrate coefficient of friction, Ti/Ti-DLC and Ti/AlTiN/Ti-DLC coatings with the values of 0.44, 0.1 and 0.1. The friction coefficient of Ti/Ti-DLC and Ti/AlTiN/Ti-DLC coatings did not show any obvious change after 1 hour wear testing, while the friction coefficient of Ti/Ti-DLC coatings shows an increase because of coating partial delamination.

Adhesion is one of the most important coating properties, and can be assessed with the scratch test. The problem with this method is defining the critical lateral and normal forces. Fig. 5(a) and (b) shows the lateral force and normal force change during a typical scratch test of the Ti/Ti-DLC and Ti/AlTiN/Ti-DLC coatings. The critical lateral load is easily identified from the slope variations. The normal force was increased linearly during the scratch testing, so it was easily calculated

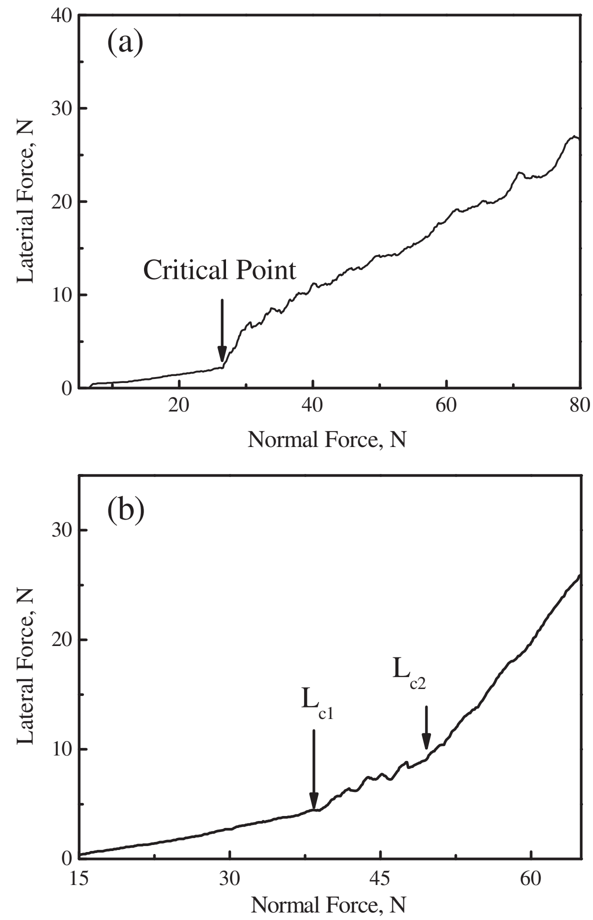

Fig. 5. Scratch test of (a) Ti/Ti-DLC and (b) Ti/AlTiN/Ti-DLC coatings.

at the critical coating delamination. Fig. 5(a) shows the critical point of delamination of the Ti/Ti-DLC coatings from the substrate, which is about 26.5 N. The DLC/AlTiN coating exhibits two critical loads, L_{c1} = 38.2 N and L_{c2} = 47.8 N. The critical normal load obviously increases with the AlTiN layer introduction. The main reason is that the supporting AlTiN layer affected the DLC coating, demonstrated by the decrease in the hardness of the DLC layer. The other reason is the supporting AlTiN layer enhanced the coating deformation resistance under the scratch tip. The critical normal load also decreased because of the lower film thickness. The challenge lies in developing a method to produce these coatings with high hardness and wear resistance, while at the same time not sacrificing adhesion strength. This challenge can be solved by using the proper metallic interlayer or supporting layer and optimizing its thickness.

Tribological and adhesion properties of the Ti/Ti-DLC and Ti/AlTiN/Ti-DLC coatings are presented in Figs. 4 and 5. Both tribological and adhesion properties differ because of the AlTiN supporting layer under DLC films. The main reason is that the stress including intrinsic stress and deformation stress can be effectively released in different layers' interfaces, so the high wear resistance and adhesion can be expected, which were verified in Figs. 4 and 5.

4. Conclusions

Ti/Ti-DLC and Ti/AlTiN/Ti-DLC composite coatings were deposited by magnetron sputtering on high speed steel W18Cr4V substrates. Ti and AlTiN interlayers have a columnar structure with 50–80 nm grain size. Ti/Ti-DLC coating hardness is about 25.9 ± 0.4 and their elastic modulus is 222.2 ± 6.3 GPa, whereas for Ti/AlTiN/Ti-DLC composite coatings corresponding hardness and modulus values are 19.3 ± 1.0

and 205.6 ± 6.7 GPa, respectively. Adhesion of Ti-DLC coating with the substrate expressed as the critical lateral force is about 26.5 N, but adhesion of Ti/AlTiN/Ti-DLC and substrate is about 38.2 N, and adhesion of AlTiN and Ti-DLC is about 47.8 N. Friction coefficient of the substrate without coating is 0.44, and it is 0.1 with Ti/Ti-DLC and Ti/AlTiN/Ti-DLC coatings, although the wear resistance of the Ti/AlTiN/Ti-DLC composite coatings is much higher than the Ti/Ti-DLC coatings because of the AlTiN supporting layer releasing the internal and deformation stresses.

Acknowledgments

This work was supported by the China State Key Lab of Advanced Metals and Materials and the National Nature Science Foundation of China (51001013).

References

[1] X. Pang, K. Gao, F. Luo, Y. Emirov, A.A. Levin, A.A. Volinsky, Thin Solid Films 517 (2009) 1922.
[2] B. Segura-Giraldo, E. Restrepo-Parra, P.J. Arango-Arango, Appl. Surf. Sci. 256 (2009) 136.
[3] R.K. Singh, Z.H. Xie, A. Bendavid, P.J. Martin, P. Munroe, M. Hoffman, Diamond Relat. Mater. 17 (2008) 975.
[4] M. Sedlacek, B. Podgornik, J. Vizintin, Mater. Charact. 59 (2008) 151.
[5] T. Takeno, T. Sugawara, H. Miki, T. Takagi, Diamond Relat. Mater. 18 (2009) 1023.
[6] K.-R. Lee, K.Y. Eun, I. Kim, J. Kim, Thin Solid Films 377/378 (2000) 261.
[7] K.-W. Chen, J.-F. Lin, Thin Solid Films 517 (2009) 4916.
[8] L.F. Bonetti, G. Capote, L.V. Santos, E.J. Corat, V.J. Trava-Airoldi, Thin Solid Films 515 (2006) 375.
[9] T. Michler, C. Siebert, Surf. Coat. Technol. 163 (164) (2003) 546.
[10] Y.T. Pei, X.L. Bui, X.B. Zhou, J.Th.M. De Hosson, Surf. Coat. Technol. 202 (2008) 1869.
[11] S.J. Harris, A.M. Weiner, W.-J. Meng, Wear 211 (1997) 208.
[12] T.W. Scharf, J.A. Ohlhausen, D.R. Tallant, S.V. Prasad, J. Appl. Phys. 101 (2007) 63521.
[13] J. Takadoum, H. Houmid Bennani, M. Allouard, Surf. Coat. Technol. 88 (1997) 232.
[14] C. Strondl, G.J. van der Kolk, T. Hurkmans, W. Fleischer, T. Trinh, N.M. Carvalho, J.Th.M. de Hosson, Surf. Coat. Technol. 142 (144) (2001) 707.
[15] C. Strondl, N.M. Carvalho, J.Th.M. De Hosson, G.J. van der Kolk, Surf. Coat. Technol. 162 (2003) 288.
[16] W.H. Kao, Y.L. Su, S.H. Yao, H.C. Huang, Surf. Coat. Technol. 204 (2010) 1277.
[17] M. Arndt, T. Kacsich, Surf. Coat. Technol. 163 (164) (2003) 674.
[18] X. Pang, K. Gao, A.A. Volinsky, J. Mater. Res. 22 (2007) 3531.
[19] G.S. Kim, S.Y. Lee, J.H. Hahn, B.Y. Lee, J.G. Han, J.H. Lee, S.Y. Lee, Surf. Coat. Technol. 171 (2003) 83.
[20] X. Pang, K. Gao, H. Yang, L. Qiao, Y. Wang, A.A. Volinsky, Adv. Eng. Mater. 9 (2007) 594.
[21] W.A. Landford, M.J. Rand, J. Appl. Phys. 49 (1978) 2473.
[22] H.L. Wang, M.J. Chiang, M.H. Hon, Ceram. Int. 27 (2001) 383.
[23] H. Buckle, in: J.W. Westbrook, H. Conrad (Eds.), The Science of Hardness Testing and Its Research Applications, American Society for Metals, Metals Park, OH, 1973, p. 453.
[24] C. Casiraghi, A.C. Ferrari, J. Robertson, Phys. Rev. B 72 (2005) 085401.
[25] J. Robertson, Mater. Sci. Eng. R 37 (2002) 129.